Investigation of Landing Gear Alternatives for High Performance Aircraft

A. R. DeWispelare* and R. P. Stager†
Air Force Institute of Technology, WPAFB, Ohio

In an effort to improve rough field performance for a specific high performance aircraft, the modeling of runway profiles, the aircraft structure, landing gears, and aerodynamics was accomplished. Various load alleviation schemes are modeled and then combined with the aforementioned runway and aircraft models into a dynamic simulation which allows the evaluation of the control schemes through numeric and graphical means. These combined evaluation tools (numeric and graphic) add efficiency to the design process along with increasing physical insight into the problem. Results are presented which indicated that a number of control configurations (both passive and active) ranging in various degrees of complexity increase the rough field performance (in some cases significantly) for the selected high performance aircraft (F-16).

I. Introduction

CONVENTIONAL landing gear designs which minimize rolling moments on takeoff/landing and/or hold ground clearance approximately constant over a wide range of load configurations tend to also stress low weight and volume with the result of sacrificing rough field performance. A logical question is then, are there any types of landing gear configuration that can be retrofitted to existing high performance aircraft or designed into new aircraft which ameliorate the rough runway performance?

The goal of this effort[4] was to investigate various landing gear configurations to see which of these improved the performance of an aircraft (F-16) during ground operation on rough runways.

Approach

To determine the performance capability of the landing gear alternatives, the runway profile, aircraft airframe, aerodynamics, and landing gear are modeled as discussed in Secs. II and III. Section IV delineates alternative landing gear which are designed to attenuate vertical loads during takeoff and landing roll. The characteristics of the alternative landing gear are changed by adding forces (in the active case) or by changing the nonlinear characteristics of the strut. The models are shown to accurately represent the current F-16 structural support system in terms of dynamic response to runway inputs. The performance of the current landing gear and four alternative designs is tested by simulating the dynamic response of a fully loaded (33,500 lb) F-16 taking off from, and landing on, rough, temporarily repaired runways. Validation of the simulation was accomplished with aircraft data. The runway used simulates one with two large craters which are repaired using established rapid runway repair techniques.[1] By simulating the aircraft accelerating or decelerating over the runway with many different initial velocities, a spectrum of system responses is developed. In all cases, the accelerations and loads transmitted to the aircraft structure are calculated and compared with the aircraft's design limit loads, pylon acceleration limits, and ground clearance to determine whether any damage occurs. The implementation of this simulation is discussed in Sec. V. The overall evaluation of the load alleviation schemes was greatly facilitated by the use of graphic and numeric techniques which added efficiency to the design process along with increasing physical insight into the problem.[4]

Presented as Paper 81-1639 at the AIAA Aircraft Systems and Technology Conference, Dayton, Ohio, Aug. 11-13, 1981; submitted Sept. 18, 1981; revision received May 28, 1982. This paper is declared a work of the U.S. Government and therefore is in the public domain.

*Associate Professor, Department of Aeronautics and Astronautics.

†Graduate Student, Department of Aeronautics and Astronautics. Presently, Flight Systems Analyst, Aeronautical Systems Division (ENFZ).

II. Major Subsystem Model

Mathematical models were developed separately for each major subsystem: the airframe/aerodynamics model, the runway model, and the landing gear models. These models were then implemented in computer code and combined into a simulation to emulate the dynamic response of the aircraft.

Airframe/Aerodynamics Model

A 5-degree-of-freedom analytical model was developed based on conventional rigid body (F=mass $\times$ acceleration) analysis[3] and the following assumptions:

1) All forces defined in Fig. 1 are in the body coordinate system.
2) The rudder force in the Y direction is not considered.
3) The nose gear does not turn.
4) The aircraft will land and take off in the X-Z plane (all mats are encountered at 90 deg).
5) The Y forces entering the main gear attachment forces act in opposite directions. (The Y degree of freedom was included in order to check this assumption.)
6) A pilot model is not included.
7) Thrust acts only in the X direction of the body coordinate system.
8) Aerodynamic forces are applied at the center of gravity (c.g.).
9) Higher-order terms of angular momentum are negligible.

Yaw was not calculated since assumptions 2-7 delete the major contributors to this moment. Since it would be very difficult to model and verify what actions a pilot would take on encountering the repaired surface, assumptions 2, 3, and 6 were made.

Runway Model

The runway model (Fig. 2) was developed by modeling the repaired surface.[1] Figure 2 is a graphic representation of this surface, which is composed of a smoothed pavement and mat to cover filled-in craters.

Equation (1) was developed using Fig. 2. The output of the equation (variable Z) is the height above or below runway level. It should be mentioned that it is assumed that the

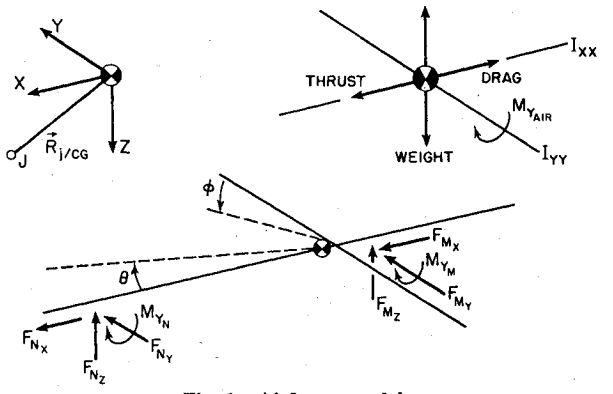

Fig. 1 Airframe model.

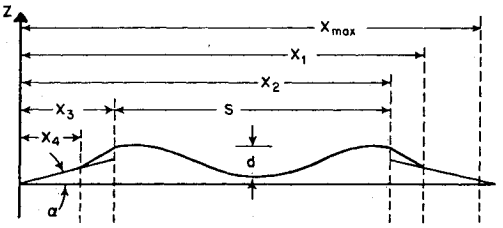

Fig. 2 Runway repair profile.

runway is mathematically flat at all times except in the proximity of a repaired area.

$$
\begin{aligned}
Z &= X\tan\alpha, && 0 < X \le X_4 \\
&= (X - X_3 + 3.75\cos\alpha)\tan(\alpha + 0.0333) \\
&\quad + (X_3 - 3.75\cos\alpha)\tan\alpha, && X_4 \le X \le X_3 \\
&= 3.75\cos\alpha\tan(\alpha + 0.0333) + (X_3 3.75\cos\alpha)\tan\alpha \\
&\quad - 0.5d\left[1 - \cos\left(2\pi\frac{X - X_3}{S}\right)\right], && X_3 \le X \le X_2 \\
&= [(X_3 + S + 3.75\cos\alpha) - X]\tan(\alpha + 0.0333) \\
&\quad + (X_3 - 3.75\cos\alpha)\tan\alpha, && X_2 \le X \le X_1 \\
&= (S + 2X_3 - X)\tan\alpha, && X_1 \le X \le X_{\max}
\end{aligned}
\tag{1}
$$

Notice that the only required input parameters are X_3, the upheaval length; α, the upheaval; S, the crater diameter; d, the mat sag; and X, the distance down the mat of the aircraft.

III. Landing Gear Models

Conventional landing gear systems, including that installed on the F-16, consist of three major elements: the shock strut, the tire, and the supporting structure. Both nose and main landing gears were modeled and analyzed in this effort although only the main gear modeling is now summarized for the sake of brevity.

Main Gear Model

The main gear system of the F-16 is a tripod arrangement. The components of the tripod are tension strut, drag brace, and two-stage piston. The strut orientation in the y-z plane is a function of strut length. The main shock strut is modeled only as a vertical load carrying element. Lateral forces are assumed canceled based on the assumption of aircraft line of travel being perpendicular to the leading and trailing edges of runway irregularities; hence, symmetrical loading is valid.

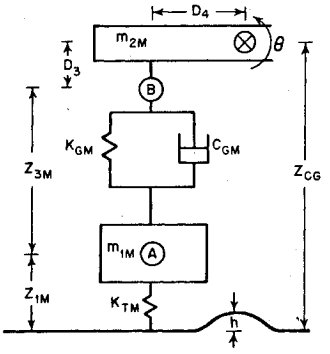

Fig. 3 Main gear model.

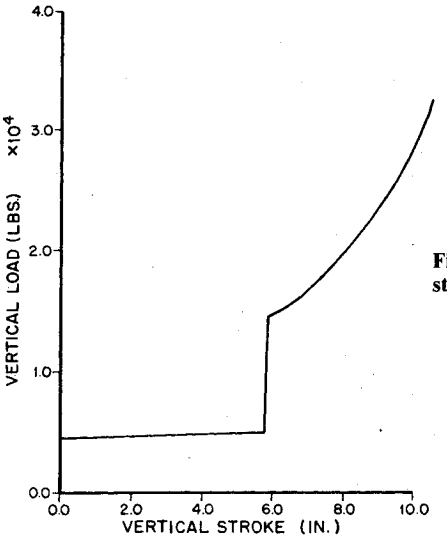

Fig. 4 Main gear load stroke curve.

The shock strut and tire determine the dynamic response of the main gear.

The shock strut is modeled as a nonlinear spring and a nonlinear damper in parallel. The tire is modeled as a nonlinear spring in series with shock strut. The unsprung mass of the main gear is lumped between the tire and shock strut. The main gear model is shown in Fig. 3, where A is the hub location, B the attachment point location, Z_{1M} the vertical displacement of the hub, Z_{3M} the vertical strut compression, K_{GM}, K_{TM}, C_{GM} the spring and damper coefficients for components, Z_{cg} the vertical displacement of the cg, h the vertical displacement of the runway, Θ the aircraft pitch angle, D_3 the vertical distance from aircraft cg to attachment point, and D_4 the horizontal distance from aircraft cg to attachment point.

The equations of motion are derived by summing forces at points A and B of Fig. 3. This yields

$$\ddot{Z}_{1M} = FKTM/m_{1M} + FCGM/m_{1M} - FKGM/m_{1M} - g \tag{2}$$

$$F_{BZ_M} = FKGM - FCGM \tag{3}$$

where $\ddot{Z}_{1M}$ is the hub vertical acceleration, $FKTM$ the main tire spring force, $FKGM$ the main shock strut spring force, $FCGM$ the main shock strut damping force, F_{BZ_M} the attachment point vertical force, m_{1M} the unsprung mass of the main gear, m_{2M} the sprung mass of aircraft, and g the gravity constant.

The main gear also provides braking during landing. The horizontal braking force (F_{BX_M}) is vertical tire force ($FKTM$) and the braking coefficient (μ).

$$F_{BX_M} = FKTM \cdot \mu \tag{4}$$

The forces shown in the above equations are characterized as follows: The spring force is described by a load-stroke

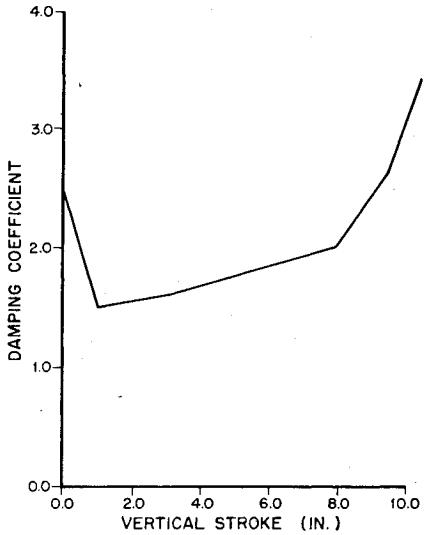

Fig. 5 Main gear damping coefficient curve.

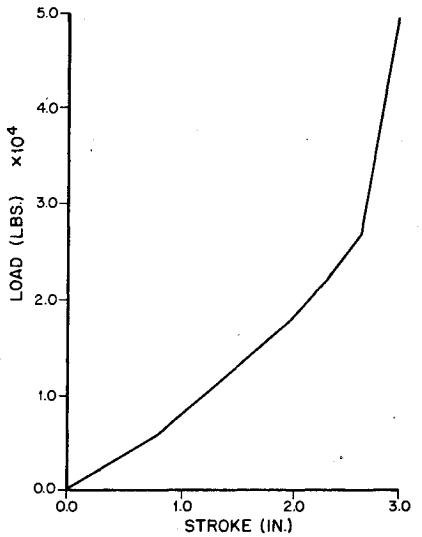

Fig. 6 Main gear tire compression curve.

curve[6] (Fig. 4). This load-stroke curve has a "discontinuity" at 5.8 in. of vertical stroke. The discontinuity is caused by the two-stage piston arrangement of the strut. The main strut, as it is being compressed from the fully extended position, has an effective area of 5.371 in.^{2}. As the vertical strut compression reaches 5.8 in., the second piston is encountered. This causes the effective area to increase to 15.904 in.^{2}. Since the load is the product of air pressure and effective area, the load "jumps" from 5000 to 14,500 lb at 5.8 in. of vertical stroke without any further strut compression. The main shock strut was designed as a two-stage piston for two reasons. First, the roll stability of the aircraft during ground operations is enhanced by allowing (in the discontinuity) a small change in strut compression for a large change in force. Second, weapon loading is made easier by ensuring that the aircraft remains a constant distance above the ground during loading. The damping force is the product of vertical strut compression velocity squared and damping coefficient. The damping coefficient, as a function of strut stroke, is shown in Fig. 5. The tire (nonlinear spring) is described by a compression curve (Fig. 6).

Rough Field Landing Gear Alternatives

Based on limited research and development programs conducted in the area of rough field operations, active and adaptive landing gear concepts appear to be most attractive for load alleviation.[2]

Active landing gear, as opposed to passive landing gear, reduce loads and accelerations transmitted to the aircraft by

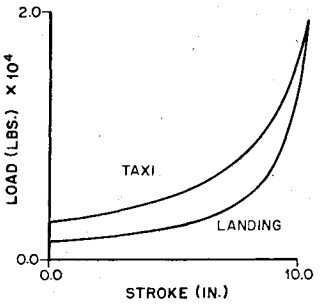

Fig. 7 Taxi and landing characteristics.

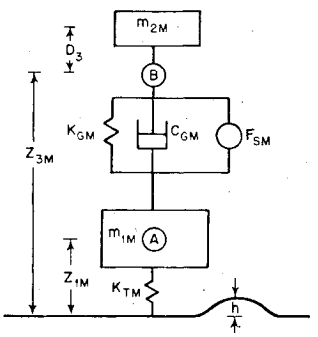

Fig. 8 Main gear parallel servo model.

applying controlled forces between the wheel/tire assembly (unsprung mass) and the aircraft (sprung mass). Various high performance aircraft which have experimented with active gear configurations in the last few years have met with limited success.[7,9] There are three basic types of active landing gear designs: 1) parallel servo, 2) series servo, and 3) servo only. The primary difference between these three active landing gear systems is the location of the active force mechanism (actuator). The series servo and servo only actuators are required to support the aircraft static weight. In the parallel servo system, a spring acting in parallel with the actuator supports the static weight. Thus the actuator need only meet the requirements of reducing the incremental loads. It has been shown that the parallel servo requires a smaller actuator and lower fluid flow rates than the series servo and servo only system.[4] A parallel servo system, therefore, seemed worthy of investigation of its feasibility with the F-16.

The adaptive gear differs from an active gear in that no mechanism applies control forces between the sprung mass and unsprung mass to reduce loads. Rather, the shock strut parameters (load-stroke curve and damping coefficient) are varied based on aircraft operating conditions. For example, these parameters can be varied as a function of aircraft response, or as a function of whether the aircraft is taking off or landing. Adaptive gear modifications are the most popular of the current load alleviation schemes. A number of operational aircraft in addition to numerous test aircraft have used one or more adaptive gear types.[3,6] There are three basic types of adaptive landing gear systems: adjustable spring constant, bandpass, and dual mode adaptive. The adjustable spring constant gear and the bandpass gear were discounted due to their lack of promise in this application. The third type of adaptive system, the dual mode adaptive gear, uses a valve between the strut and the auxiliary air chamber to connect and disconnect the auxiliary chamber depending on whether the aircraft is taxiing or landing. This results in the gear having a flatter load-stroke curve for taxi (including takeoff and landing roll-out) and changing to a conventional load-stroke curve for landing impact (Fig. 7). This adaptive gear generally applies to the main landing gear. The F-16 main landing gear was designed to operate within a discontinuity region on the load-stroke curve during taxi. The objective of the dual mode concept is to have a flatter load-stroke curve for taxiing. Therefore this design concept is not directly applicable to the F-16 main landing gear. However, a flatter load-stroke curve is found to exist for the F-16 nose gear. Therefore this concept

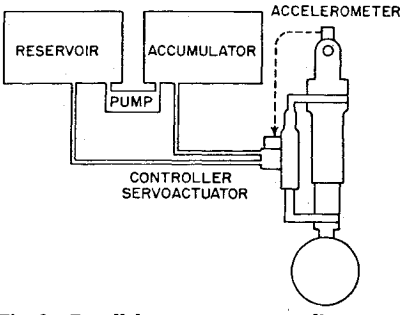

Fig. 9 Parallel servo component diagram.

has promise for the F-16, and it can be effectively implemented as a set of passive modifications to the landing gear.

IV. Alternative Landing Gear

Alternative 1—Active Gear (Parallel Servo)

The parallel servo, as described previously, reduces the forces imparted to the airframe by inputting a controlled force between the sprung and unsprung mass. Different, four state models were used for each of the nose and main gear respectively. Four states were used because this is the lowest-order system that can be used to describe a landing gear system while allowing the force at the attachment to be "controlled." The F_{SN} term is the force the actuator is exerting between the unsprung and sprung masses. The four state variables of this model are Z_{1M}, $\dot{Z}_{1M}$, Z_{3M}, and $\dot{Z}_{3M}$. The four state parallel servo model schematic for the main gear is shown in Fig. 8. The equations for the main gear parallel servo are

$$m_{1M}\ddot{Z}_{1M} = K_{TM}(L_{1M} - Z_{1M} + h) - m_{1M}g - K_{GM}[L_{2M} - (Z_{3M} - Z_{1M})] + C_{GM}(Z_{3M} - Z_{1M})\,|Z_{3M} - Z_{1M}| + F_{SM} \tag{5}$$

$$m_{2M}\ddot{Z}_{3M} = K_{GM}[L_{2M} - (Z_{3M} - Z_{1M})] - C_{GM}(Z_{3M} - Z_{1M})\,|Z_{3M} - Z_{1M}| - F_{SM} - m_{2M}g \tag{6}$$

where L_{1M} is the tire spring, unstretched length; and L_{2M} is the strut, unstretched length. It should be noted that K_{TM}, K_{GM}, and C_{GM} are not constants. They vary nonlinearly with the stroke of the tire and strut.

Since modern control theory and the methods for defining the optimal control law are well developed only for linear systems, Eqs. (5) and (6) are linearized. The main gear linearized equations are as follows:

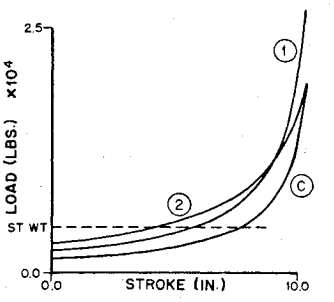

Fig. 10 Nose gear load-stroke curve.

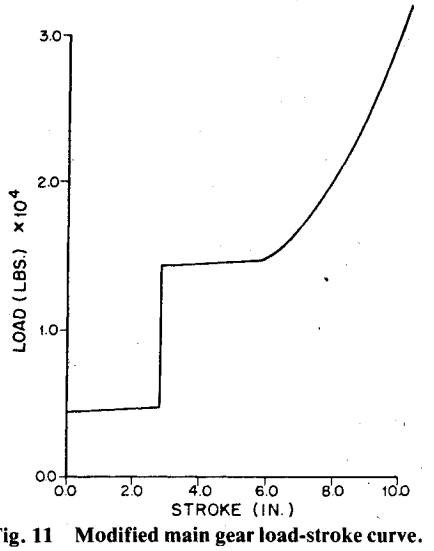

Fig. 11 Modified main gear load-stroke curve.

The equilibrium condition used is the static position of the fully loaded aircraft, where x_i are states, (δ) are perturbed quantities, and x_0 are static equilibrium conditions. An optimal control law was sought which would optimize a quadratic performance index in the perturbed state and control vector. The solution of the Riccati equation allowed the computation of the feedback gain matrix through which the control law is found as a function of state. To implement this hydraulically driven active system, the hardware components would include an actuator, servovalve, low- and high-pressure accumulation, sensors, and a controller (Fig. 9).

Alternatives 2 and 3—Nose Gear Alternatives

Two alternative nose gear concepts are described in this section. Both involve a modification of the nose gear load-stroke relationship with no change to the current main gear system. Preliminary takeoff and landing results from the simulation indicated that nose gear attachment point forces could be reduced significantly. The approach taken to reduce these forces involves increasing the remaining shock strut

$$\dot{\overline{\delta x}} = \begin{bmatrix} 0 & 1 & 0 & 0 \\ -\frac{K_{GM}}{m_{1M}} - \frac{K_{TM}}{m_{1M}} & -\frac{2C_{GM}}{m_{1M}}(x_4 - x_2) & \frac{K_{GM}}{m_{1M}} & \frac{2C_{GM}}{m_{1M}}(x_4 - x_2) \\ 0 & 0 & 0 & 0 \\ \frac{K_{GM}}{m_{2M}} & \frac{2C_{GM}}{m_{2M}}(x_4 - x_2) & -\frac{K_{GM}}{m_{2M}} & \frac{C_{GM}}{m_{2M}}(x_4 - x_2) \end{bmatrix}_{\overline{x_0}} \delta x + \begin{bmatrix} 0 \\ \frac{1}{m_{1M}} \\ 0 \\ \frac{1}{m_{2M}} \end{bmatrix}_{\overline{x_0}} \delta F_{SM} + \begin{bmatrix} 0 \\ \frac{K_{TM}}{m_{1M}} \\ 0 \\ 0 \end{bmatrix}_{\overline{x_0}} \delta h \tag{7}$$

stroke from the static condition and decreasing strut stiffness.

The two nose gear load-stroke curves investigated are shown in Fig. 10, where curve C identifies the current nose gear load-stroke curve. Curve 1 results from merely increasing the fully extended air pressure. Curve 2 results from the addition of an auxiliary air chamber to increase the air volume, coupled with increased fully extended air pressure. Both curves 1 and 2 increase the remaining stroke while curve 2 also decreases the strut stiffness. The fully extended air pressures for curves 1 and 2 are determined by the relationship of force equals pressure times area at the fully extended strut position. This results in 259.7 psia for curve C, 406.51 psia for curve 1, and 544.34 psia for curve 2. An auxiliary air chamber volume of 5.859 in.^{3} is determined from load-stroke curve 2.

Alternative 4—Modified Nose/Modified Main Gear

The objective of this alternative is to increase the amount of remaining stroke of the shock struts during ground operations. This is accomplished for the nose gear by increasing the internal pressure of the strut and using an auxiliary air chamber. One method for increasing the stroke, without losing the advantages of the two-stage piston, would be to move the stops of the second stage such that the second stage piston would be encountered sooner. The resulting load-stroke curve is shown in Fig. 11. This load-stroke curve and that of the modified 2 nose gear are used to define the modified nose/modified main alternative.

V. Validation of Computer Code

Validation of the complete simulation (RUNWAY) was accomplished with the use of two records of experimental data gathered at Edwards Air Force Base, California.[5] An F-16 test aircraft taxied over an AM-2 mat during arresting hook tests at a velocity of 155 ft/s with gross weights of approximately 27,000 and 26,000 lb, respectively. The mat was 1.5 in. high and 62 ft long with a 3.75-ft-long ramp at each end. Slightly less than 1 deg of roll is detectable in the recorded information and is used in simulating the mat encounter in RUNWAY.

To compare the data with RUNWAY simulation results, the test data was amplified in scale to several times its original size. The time-history plot of each attachment point force was traced onto corresponding plots generated using RUNWAY. The results are shown in Figs. 12 and 13. These figures demonstrate the similarity in dynamic response between the simulation and the test aircraft. Comparing maximum forces between the simulation and real data indicates a 40.8% difference for the nose gear. A relatively close approximation to the actual data is obtained for the right and left main gear with differences of 0.2 and 7.3%, respectively.

The disparity for the nose gear is attributed to the lack of recorded action of the pilot, flap settings, and elevator settings that can lessen the impact on the nose gear during encounters with the mat. The high frequency vibration present in the RUNWAY generated responses for the main gear is attributed to the discontinuity in the load stroke curve (Fig. 4). In the simulation, this vertical discontinuity was approximated by a 0.02-in. stroke for the jump from 5000 to 14,500 lb of vertical load. Other slopes for the vertical discontinuity were used during simulation, and the frequency and magnitude of this vibration were changed. Therefore this vibration was considered insignificant compared to the gear dynamics.

Takeoff Distance Test

Simulation results of a 33,500-lb aircraft are compared with actual test results.[5] Figure 14 shows that the two independent simulations differ by 3.3% when comparing distances and by 3.0% when comparing velocities at the same point. Similarly, results differ by 0.3 and 4.5% for the liftoff distance and velocity, respectively, for a 33,500-lb aircraft.[8] During the takeoff analysis, the lateral displacement did not exceed 2 ft.

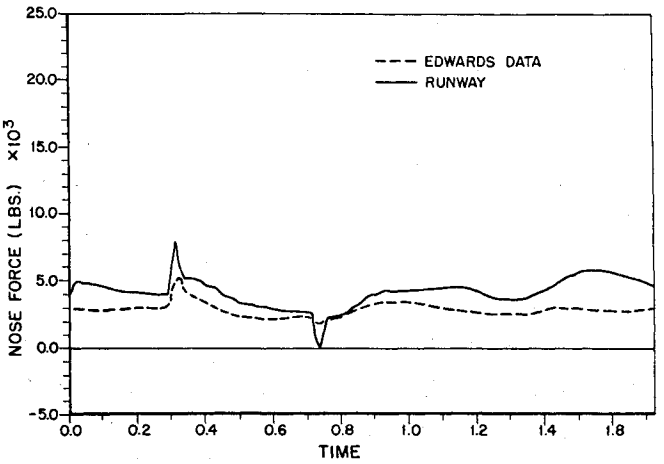

Fig. 12 Nose gear response comparison.

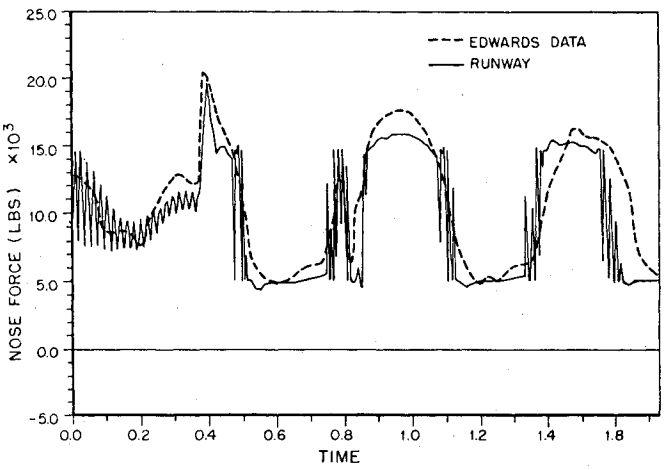

Fig. 13 Main gear response comparison.

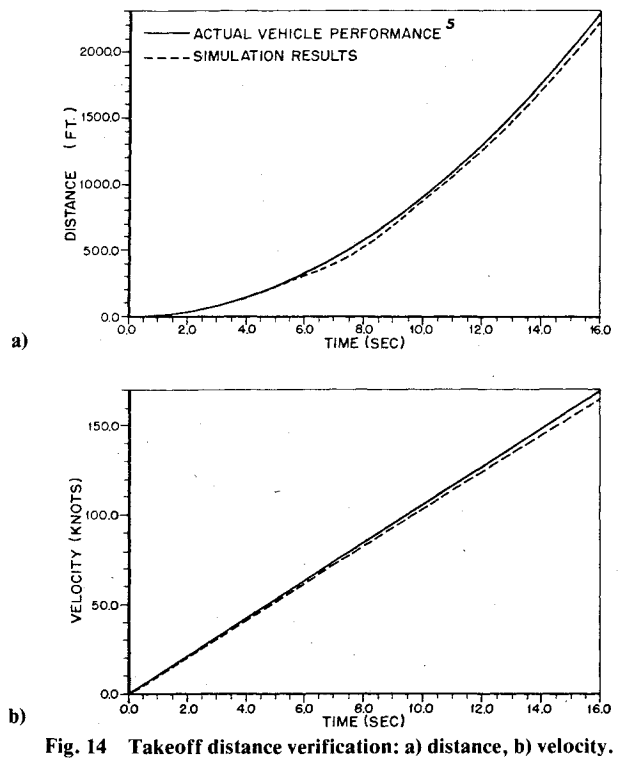

Fig. 14 Takeoff distance verification: a) distance, b) velocity.

Table 1 Failure occurrence—current gear

		Repair A							Repair B								
Mode	Speed	NT	MT	NDL	MDL	SL	PS	GC	NT	MT	NDL	MDL	SL	PS	GC	*F*	*S*
Takeoff	20			23.0					X						1.47	2	0
	40							1.57								1	1
	60			21.1	37.9						23.2				1.52	2	0
	80			20.2	37.2			1.28			22.4	33.3			1.55	2	0
	100							0.80				34.0				2	0
	120															0	2
	140															0	2
	160			20.2								36.0				2	0
	180			24.1	33.4											1	1
	200				31.1							31.2				2	0
	220				34.7							34.6				2	0
	240				37.6							37.9				2	0
	260			20.6	39.2						21.2	47.5			0.91	2	0
	280			19.8	46.6						19.8	74.8				2	0
Landing	40															0	2
	60															0	2
	80															0	2
	100			21.5												1	1
	120															0	2
	140															0	2
	160															0	2
	180															0	2
	200															0	2
	220			45.8												1	1
															Total	24	24

Table 2 Failure occurrence—active gear

		Repair A							Repair B								
Mode	Speed	NT	MT	NDL	MDL	SL	PS	GC	NT	MT	NDL	MDL	SL	PS	GC	*F*	*S*
Takeoff	20															0	2
	40															0	2
	60															0	2
	80															0	2
	100															0	2
	120															0	2
	140															0	2
	160															0	2
	180															0	2
	200															0	2
	220															0	2
	240										32.1					1	1
	260			20.6	38.2						42.1					2	0
	280				39.9						41.9					2	0
Landing	40															0	2
	60															0	2
	80															0	2
	100															0	2
	120															0	2
	140															0	2
	160															0	2
	180															0	2
	200															0	2
	220															0	2
															Total	5	43

This would tend to support our assumptions that lateral displacement of the aircraft is negligible.

VI. Results

The aforementioned models were combined into a simulation which used the runway profile as input. The runway profile used contained two repairs each 90 ft long and separated by 100 ft of undamaged runway. Each repair is covered by a mat[1] which extends over the 70-ft-diam crater with 10 ft of pavement upheaval at the ends of the mat. A 2.5-in. (repair A) or 1.0-in. sag (repair B) is inserted at the midpoint of each mat to simulate soil compaction as the runway is used. To add realism to the runs, the aircraft is accelerated on takeoff using initial velocities prior to encountering the repairs between 20 and 280 ft/s in 20-ft/s increments, and the aircraft is decelerated on landing between 40 and 220 ft/s for each of the current and alternative gear. The system success or failure is output for each run. The results of all the runs are shown in Tables 1-5 and summarize the nature of failure indicated by each computer run.[3] Familiarization with the following is helpful when referring to

Table 3 Failure occurrence—modified nose gear 1

		Repair A							Repair B								
Mode	Speed	NT	MT	NDL	MDL	SL	PS	GC	NT	MT	NDL	MDL	SL	PS	GC	*F*	*S*
Takeoff	20															0	2
	40															0	2
	60			19.6	32.0			1.6								1	1
	80				35.0							36.3				2	0
	100											34.3			1.34	1	1
	120															0	2
	140															0	2
	160											36.4				1	1
	180				36.5											1	1
	200				31.2							31.2				2	0
	220				34.5							34.5				2	0
	240				37.9							38.4				2	0
	260				38.8							40.2				2	0
	280				45.0							42.9				2	0
Landing	40															0	2
	60															0	2
	80															0	2
	100															0	2
	120															0	2
	140															0	2
	160															0	2
	180															0	2
	200															0	2
	220															0	2
															Total	16	32

Table 4 Failure occurrence—modified nose gear 2

		Repair A							Repair B								
Mode	Speed	NT	MT	NDL	MDL	SL	PS	GC	NT	MT	NDL	MDL	SL	PS	GC	*F*	*S*
Takeoff	20															0	2
	40															0	2
	60															0	2
	80				32.8							36.4				2	0
	100											33.9				1	1
	120															0	2
	140															0	2
	160											36.0				1	1
	180				37.1											1	1
	200				30.8							31.0				2	0
	220				34.2							34.3				2	0
	240				37.1							42.8				2	0
	260				44.0							70.0				2	0
	280				60.0							105.0				2	0
Landing	40															0	2
	60															0	2
	80															0	2
	100															0	2
	120															0	2
	140															0	2
	160			19.8												1	1
	180															0	2
	200															0	2
	220															0	2
															Total	16	32

these tables. MODE refers to landing or takeoff. SPEED refers to the speed (in feet per second) of the accelerating aircraft 20 ft before encountering the repair. NT is the nose gear tire failure (fully compressed tire). MT is the main gear tire failure (fully compressed tire). NDL is the nose gear design limit load exceeded (19.4×10^3 lb); values given are in $(10)^3$ lb. MDL is the main gear design limit load exceeded (30.3×10^3 lb); values given are in $(10)^3$ lb. SL is the design limit load exceeded at stores location. PS is the failure due to excessive acceleration at the pilot station (3 Hz and 6 gs). GC is the minimum allowable ground clearance exceeded (+1.67 in.). *F* is the number of failures. *S* is the number of successes.

The majority of failures resulted from loads exceeding the structural design limits for the main and nose gear. Table 6 summarizes the results of the runs. All gear performed better on landing because the landing simulations were run with an unloaded F-16 (17,500 lb) contrasted with a fully loaded F-16 (33,500 lb) on takeoff.

These results of the simulation indicate that the active gear provides the best force attenuation capability. It can be seen that the modified nose/modified main is very close to the active gear in capability. This shows that significant load alleviation improvements can be achieved by changing to alternative gear.

Table 5 Failure occurrence—modified nose/modified main gears

Mode	Speed	Repair A NT	MT	NDL	MDL	SL	PS	GC	Repair B NT	MT	NDL	MDL	SL	PS	GC	F	S
Takeoff	20															0	2
	40															0	2
	60															0	2
	80															0	2
	100															0	2
	120															0	2
	140															0	2
	160															0	2
	180															0	2
	200				32.2											1	1
	220											30.6				1	1
	240				33.1							35.5				2	0
	260				37.6							56.8				2	0
	280				41.6							78.9				2	0
Landing	40															0	2
	60															0	2
	80															0	2
	100															0	2
	120															0	2
	140															0	2
	160															0	2
	180															0	2
	200															0	2
	220															0	2
															Total	8	40

Table 6 Alternative gear capability summary (capability values given are for a repaired runway; capability for a smooth runway is assumed to equal 1)

Landing gear alternatives	Failures	Successes	Capability
Current	24	24	0.5000
Active	5	43	0.8958
Modified nose 1	16	32	0.6667
Modified nose 2	16	32	0.6667
Modified nose/main	8	40	0.8333

While other performance measures such as reliability and cost are not described in this paper, one would need to consider them when making a decision on gear goodness.[4]

Pilot station accelerations were considered in this effort, but it was found that all the gear investigated attenuated these accelerations below critical values.

VII. Summary

The objective, of all alternatives investigated in this study, is to reduce attachment point loads. Four alternative gear concepts are developed, which include one active gear (the parallel servo) and three passive modifications. All four of these gear improve performance of the F-16 on rough/repaired runways when compared to the F-16 with its current gear. Two of the passive modifications pertain to the nose gear while the third considers modification to both the nose and main gear. The active alternative reduces these loads through the use of an actuator. The three passive modifications reduce the loads by changing load-stroke curve to allow more stroke from a static to a fully compressed state. The active gear would require an accelerometer, analog computer, actuator, controller, and servovalve. One passive nose alternative requires no external modification. The load-stroke curve of this alternative results from increasing the internal air pressure. The other passive nose alternative requires an auxiliary air chamber and an increased internal air pressure. The final passive alternative uses the second passive nose alternative in conjunction with moving the second-stage piston of the main gear.

The analysis has shown that two of the alternatives significantly improve landing gear and hence aircraft performance on rough/repaired runways. The active gear alternative and the modified nose/main gear alternative increased performance 79 and 66%, respectively.

Among the conclusions to be drawn from this effort are the following: landing gear can be designed to significantly improve the F-16 capability to operate on rough/repaired runways, but this capability is sensitive to aircraft weight, velocity, and pavement upheaval; and computer generated numeric and graphic aids greatly facilitate the design and analysis in a dynamic response problem like landing gear design.

References

[1] "Rapid Runways Repair Policy," Air Force Regulation 93-2, Department of the Air Force, Washington, D.C., 1972.

[2] "Rough/Soft Field Landing Gear Technology," Air Force Wright Aeronautical Laboratories/FIEM, Wright-Patterson AFB, Ohio, 1979.

[3] Burkhardt, T.H. and Wilson, E.G. Jr., "F-4 Response to Ground Induced Loads," McDonnell Douglas Aircraft Co., June 1979.

[4] Stager, A.P. et al., "Investigation of F-16 Landing Gear Alternatives for Operation on Repaired Bomb Damaged Runways," GSE-80D Design Study, Air Force Institute of Technology, 1980.

[5] "F-16 Taxi Data for Air Force Civil Engineering Environmental Development Office," General Dynamics, AF/CEEDO, 1978.

[6] "YF-16 Dynamic Loads Analysis," General Dynamics, SDR-401-005, 1973.

[7] Ross, I. and Edson, R., "An Electronic Control for an Electrohydraulic Active Control Aircraft Landing Gear," Hydraulic Research Division of Textron, Inc., NASA Contract NAS1-14459, Jan. 1979.

[8] *Supplement Flight Manual (U)*, Technical Order 1F-16A-1-1, F-16A/B Series, April 13,1979.

[9] Wignot, J.E., Durup, P.C., and Gamon, M.A., *Design Formulation and Analysis of an Active Landing Gear*, Vol. I—Analysis, AFFDL-TR-71-80, 1971.